Flat topped beams and their characteristics in turbulent media

Halil Tanyer Eyyuboğlu, Çağlar Arpali and Yahya Baykal

*Çankaya University, Electronic and Communication Engineering Department,
Öğretmenler Cad. No: 14 Yüzüncüyıl 06530 Balgat Ankara, Turkey.*
h.eyyuboglu@cankaya.edu.tr, c.arpali@cankaya.edu.tr, y.baykal@cankaya.edu.tr

Abstract: The source and receiver plane characteristics of flat topped (FT) beam propagating in turbulent atmosphere are investigated. To this end, source size, beam power and M^2 factor of source plane FT beam are derived. For a turbulent propagation medium, via Huygens Fresnel diffraction integral, the receiver plane intensity is found. Power captured within an area on the receiver plane is calculated. Kurtosis parameter and beam size variation along the propagation axis are formulated. Graphical outputs are provided displaying the variations of the derived source and receiver plane parameters against the order of flatness and propagation length. Analogous to free space behavior, when propagating in turbulence, the FT beam first will form a circular ring in the center. As the propagation length increases, the circumference of this ring will become narrower, giving rise to a downward peak emerging from the center of the beam, eventually turning the intensity profile into a pure Gaussian shape.

OCIS codes: (010.1330) Atmospheric turbulence, (010.1300) Atmospheric propagation, (010.3310) Laser beam transmission, (010.1290) Atmospheric optics

---

References and links

1. F. M. Dickey and S. C. Holswade, *Laser beam shaping*: *theory and techniques* (Marcel Dekker, New York, 2000).
2. D. L. Shealy and J. A. Hoffnagle, "Beam shaping profiles and propagation," in *Laser Beam Shaping VI*, F. M. Dickey and D. L. Shealy, eds., Proc. SPIE **5876**, 1-11 (2005).
3. Y. Li, "Light beams with flat-topped profiles," Opt. Lett. **27**, 1007-1009 (2002).
4. Y. Li, "New expressions for flat-topped light beams," Opt. Commun. **206**, 225-234 (2002).
5. F. Gori, "Flattened Gaussian beams," Opt. Commun. **107**, 335-341 (1994).
6. Y. Baykal and H. T. Eyyuboğlu, "Scintillation index of flat-topped-Gaussian beams," Appl. Opt. **45** (2006).
7. X. Ji and B. Lü, "Propagation of a flattened Gaussian beam through multi-apertured optical *ABCD* systems," Optik **114**, 394-400 (2003).
8. Y. Cai and Q. Lin, "Light beams with elliptical flat-topped profiles," J. Opt. A: Pure Appl. Opt. **6**, 390-395 (2004).
9. Y. Cai and Q. Lin, "A partially coherent elliptical flattened Gaussian beam and its propagation," J. Opt. A: Pure Appl. Opt. **6**, 1061-1066 (2004).
10. V. Bagini, R. Borghi, F. Gori, M. Santarsiero, D. Ambrosini, and G. S. Spagnolo, "Propagation of axially symmetric flattened Gaussian beams," J. Opt. Soc. Am. A **13**, 1385-1394 (1996).
11. N. Zhou, G. Zeng, and L. Hu, "Algorithms for flattened Gaussian beams passing through apertured and unapertured paraxial *ABCD* optical systems," Opt. Commun. **240**, 299-306 (2004).
12. B. Lü and S. Lou, "General propagation equation of flattened Gaussian beams," J. Opt. Soc. Am. A.**17**, 2001-2004 (2000).
13. B. Lü and H. Ma, "Coherent and incoherent off-axial Hermite-Gaussian beam combinations," Appl. Opt. **39**, 1279-1289 (2000).
14. D. Ge, Y. Cai, and Q. Lin, "Partially coherent flat-topped beam and its propagation," Appl. Opt. **43,** 4732-4738 (2004).

15. J. Zhang and Y. Li, "Atmospherically turbulent effects on partially coherent flat-topped Gaussian beam," in *Optical Technologies for Atmospheric, and Environmental Studies,* D. Lu and G. G. Matvienko, eds., Proc. SPIE **5832**, 48-55 (2005).
16. W.H. Carter, "Spot size and divergence for Hermite Gaussian beams of any order," Appl. Opt. **19,** 1027-1029 (1980).
17. H. T. Eyyuboğlu and Y. Baykal, "Hermite-sine-Gaussian and Hermite-sinh-Gaussian laser beams in turbulent atmosphere," J. Opt. Soc. Am. A **22,** 2709-2718 (2005).
18. H. Mao, D. Zhao, F. Jing, and H. Liu, "Propagation characteristics of the kurtosis parameters of flat-topped beams passing through fractional Fourier transformation systems with a spherically aberrated lens," J. Opt. A: Pure Appl. Opt. **6,** 640-650 (2004).
19. J. E. Harvey and J. L. Forgham, "The spot of Arago: New relevance for an old phenomenon," Am. J. Phys. **52**, 243-247 (1984).
20. Y. Cai and S. He "Average intensity and spreading of an elliptical Gaussian beam in a turbulent atmosphere," Opt. Lett. **31**, 568-570 (2006).
21. Y. Cai and S. He "Propagation of various dark hollow beams in a turbulent atmosphere," Opt. Express **14**, 1353-1367 (2006).

1. Introduction

Flat topped (FT) beams are derived from the fundamental Gaussian beam by introducing an order of flatness parameter. They possess a number of attractive features. Amongst these are less spreading in propagation and medical applications [1]. It is the former that is of interest to us in this article. From propagation point of view, there exists a wide selection of source beam formulations. Broadly considered, four basic classifications are possible, namely, super-Gaussian, flattened-Gaussian, Fermi-Dirac and super-Lorentzian [2, 3]. Among these, our model is based on flattened-Gaussian beam of Li [3, 4] which consists of taking the original flattened-Gaussian case proposed by Gori [5] and including the Gaussian exponential inside the summation after applying the conditions of flatness. In all cases however, there is an order parameter whose role is to control the flatness of the beam.

Recently we have analyzed the scintillation properties of flattened-Gaussian type beams, concluding that it will have favorable characteristics at certain propagation ranges, source sizes and operating wavelengths [6].

Up to now, some studies have been conducted by Cai, Lü and other researchers, mainly exploiting the free space propagation aspects of FT beams [7-14]. Very few studies concerning propagation in atmospheric turbulence have appeared in the literature [15]. On the other hand a comprehensive analysis of the source and the receiver plane parameters of FT beams in the presence of atmospheric turbulence have not so far been undertaken. In this respect, our current study has the following novelties

    1. The inclusion of turbulence in the propagation of FT beams
    2. A comprehensive analysis of source and receiver plane parameters of FT beams.

2. Formulation

2.1. Formulation of the source field and its related parameters

Our source field expression is adopted from Eq. (8) of [3], by dropping the order parameter in the denominator. Hence the field expression, $u_s(\mathbf{s})$ becomes

$$u_s(\mathbf{s}) = u_s\left(s_x, s_y\right) = 1 - \left[1 - \exp\left(-s_x^2/\alpha_{sx}^2 - s_y^2/\alpha_{sy}^2\right)\right]^N, \qquad (1)$$

in Eq. (1), $\left(s_x, s_y\right)$ designates the decomposition of the vector $\mathbf{s}$ into x and y components of the transverse source plane, N is the order parameter for flatness, such that at $N = 1$, $u_s(\mathbf{s})$ will yield the fundamental mode (Gaussian) source field, correspondingly α_{sx} and α_{sy} becoming the Gaussian source sizes along s_x and s_y directions. When $N \neq 1$, on the other hand, the beam sizes will depart from Gaussian source sizes, and according to the definition developed by Carter [16], will be given by

$$\alpha_{sxN} = \left[2 \int\limits_{-\infty}^{\infty} \int\limits_{-\infty}^{\infty} s_x^2 I_s(\mathbf{s}) ds_x ds_y \bigg/ \int\limits_{-\infty}^{\infty} \int\limits_{-\infty}^{\infty} I_s(\mathbf{s}) ds_x ds_y \right]^{1/2}, \tag{2}$$

$$\alpha_{syN} = \left[2 \int\limits_{-\infty}^{\infty} \int\limits_{-\infty}^{\infty} s_y^2 I_s(\mathbf{s}) ds_x ds_y \bigg/ \int\limits_{-\infty}^{\infty} \int\limits_{-\infty}^{\infty} I_s(\mathbf{s}) ds_x ds_y \right]^{1/2}, \tag{3}$$

where, $I_s(\mathbf{s})$ denotes the intensity of the source plane to be obtained from Eq. (1) as follows

$$I_s(\mathbf{s}) = u_s(\mathbf{s}) u_s^*(\mathbf{s}). \tag{4}$$

Hence upon substitution into Eq. (2) from Eqs. (1) and (4), and expanding the terms in the square bracket as binomial series, thus performing the integrations, beam size of the s_x direction will read

$$\alpha_{sxN} = \alpha_{sx} \left[2 \sum_{n=1}^{N} \sum_{n_1=1}^{N} (-1)^{n+n_1} \binom{N}{n}\binom{N}{n_1} \frac{1}{(n+n_1)^2} \bigg/ \sum_{n=1}^{N} \sum_{n_1=1}^{N} (-1)^{n+n_1} \binom{N}{n}\binom{N}{n_1} \frac{1}{(n+n_1)} \right]^{1/2}, \tag{5}$$

where the forms of $\binom{C_1}{C_2}$ refer to binomial coefficients such that, $\binom{C_1}{C_2} = C_1! / \left[(C_1 - C_2)! \, C_2! \right]$. In Eq. (5), the expression for α_{syN} is attained by simply interchanging α_{sx} with α_{sy}. From Eq. (5), it is clear that at $N = 1$, α_{sxN} will appropriately reduce to α_{sx}.

The power contained in the FT beam of flatness order N, denoted as P_{sN}, can be calculated by integrating the intensity over the entire transverse plane, which means that it is equivalent to the denominator in Eqs. (2) or (3). This way P_{sN} will become

$$P_{sN} = 2\pi \alpha_{sx} \alpha_{sy} \sum_{n=1}^{N} \sum_{n_1=1}^{N} (-1)^{n+n_1} \binom{N}{n}\binom{N}{n_1} \frac{1}{(n+n_1)}. \tag{6}$$

M^2 is reported to be a measure of beam quality [13]. Its formulation, again separated into s_x and s_y components, is given by

$$M_x^2 = 4\pi \left(\sigma_{sx}^2 \sigma_{fx}^2 \right)^{0.5}, \tag{7}$$

$$M_y^2 = 4\pi \left(\sigma_{sy}^2 \sigma_{fy}^2 \right)^{0.5}, \tag{8}$$

where the pairs σ_{sx}^2 and σ_{sy}^2, σ_{fx}^2 and σ_{fy}^2 are respectively, the second moments associated with spatial and frequency spatial domains that are described, for the x direction, by the following equations

$$\sigma_{sx}^2 = \frac{\int\limits_{-\infty}^{\infty} s_x^2 I_s(s_x) ds_x}{\int\limits_{-\infty}^{\infty} I_s(s_x) ds_x}, \tag{9}$$

$$\sigma_{fx}^2 = \frac{\int\limits_{-\infty}^{\infty} f_x^2 I_f\left(f_x\right) df_x}{\int\limits_{-\infty}^{\infty} I_f\left(f_x\right) df_x}. \tag{10}$$

Here the f_x and f_y are the variables of frequency spatial domain. $I_s\left(s_x\right)$ and $I_f\left(f_x\right)$ are attained by respectively decoupling the x and y components in the manner $I_s\left(s_x,s_y\right) = I_s\left(s_x\right)I_s\left(s_y\right)$, $I_f\left(f_x,f_y\right) = I_f\left(f_x\right)I_s\left(f_y\right)$ where the function, $I_f\left(f_x,f_y\right)$, is retrieved from the two dimensional spatial frequency Fourier transform of $I_s\left(s_x,s_y\right)$. Identical expressions will hold for the y component. By applying the same steps as before, that is resorting to the use of binomial expansion, the M_x^2 of Eq. (7) will develop into

$$M_x^2 = 2\left[\frac{\sum_{n=1}^{N}\sum_{n_1=1}^{N}(-1)^{n+n_1}\binom{N}{n}\binom{N}{n_1}\left(\frac{(nn_1)}{(n+n_1)^3}\right)}{\sum_{n=1}^{N}\sum_{n_1=1}^{N}(-1)^{n+n_1}\binom{N}{n}\binom{N}{n_1}\frac{1}{(n+n_1)}}\right]^{1/2}. \tag{11}$$

Note that M_y^2 will be identical to M_x^2. Thus, both M_x^2 and M_y^2 carry no dependency on the source parameters involving the transverse directions. Furthermore, the definition of M^2 is confined to the source plane, therefore for an FT beam considered in this paper, Eq. (11) will be valid regardless of propagation medium.

Before ending this section, we would like to note that, although it is theoretically possible to have selected N to be non-integer as pointed out by Li [4], we limit the present study to N being (positive) integer, since, the summations would otherwise turn into infinite series, thus preventing us gaining a proper insight into the subject.

2.2. Formulation of the average receiver intensity and its related parameters

After the FT beam has propagated in the turbulent atmosphere, the average intensity on a receiver plane located at axial distance of L away from the source plane, will be supplied via the Huygens Fresnel integral in the following way

$$<I_r(\mathbf{p})>=<I_r\left(p_x,p_y\right)>=\frac{k^2}{(2\pi L)^2}\int\limits_{-\infty}^{\infty}\int\limits_{-\infty}^{\infty}\int\limits_{-\infty}^{\infty}\int\limits_{-\infty}^{\infty}d^2s_1 d^2s_2 u_s(\mathbf{s}_1)u_s(\mathbf{s}_2)\exp\left\{jk\frac{\left[(\mathbf{p}-\mathbf{s}_1)^2-(\mathbf{p}-\mathbf{s}_2)^2\right]}{2L}\right\}$$
$$\times<\exp\left[\psi(\mathbf{s}_1,\mathbf{p})+\psi^*(\mathbf{s}_2,\mathbf{p})\right]>, \tag{12}$$

where $(\mathbf{p})=\left(p_x,p_y\right)$ are the x and y components of the transverse receiver plane, $k=2\pi/\lambda$ with λ being the wavelength of propagation. The ensemble average term appearing on the second line of Eq. (12) is [17]

$$<\exp\left[\psi(\mathbf{s}_1,\mathbf{p})+\psi^*(\mathbf{s}_2,\mathbf{p})\right]>=\exp\left[-0.5D_\psi(\mathbf{s}_1-\mathbf{s}_2)\right]=\exp\left[-\rho_0^{-2}(\mathbf{s}_1-\mathbf{s}_2)^2\right], \tag{13}$$

where $D_\psi\left(\mathbf{s}_1 - \mathbf{s}_2\right)$ represents the wave structure function, and $\rho_0 = \left(0.545\, C_n^2 k^2 L\right)^{-3/5}$ is the coherence length of a spherical wave propagating in the turbulent medium, C_n^2 indicates the structure constant. As expressed in Eq. (13), in our derivation we employ the quadratic approximation of Rytov's phase structure function.

When the source field expression of Eq. (1) is substituted into Eq. (12), thereby benefiting from the term by term integration facility invoked by the use of binomial expansion, the average receiver intensity takes the form of

$$
<I_r(p)> = 1 - \sum_{n=0}^{N}(-1)^n \binom{N}{n}\frac{\beta\alpha_{sx}\alpha_{sy}}{\left(\zeta_{nx}\zeta_{ny}\right)^{1/2}}\exp\left(-\frac{\beta_n p_x^2}{2\zeta_{nx}}-\frac{\beta_n p_y^2}{2\zeta_{ny}}\right) - \sum_{n=0}^{N}(-1)^n\binom{N}{n}\frac{\beta\alpha_{sx}\alpha_{sy}}{\left(\zeta_{nx}^*\zeta_{ny}^*\right)^{1/2}}\exp\left(-\frac{\beta_n p_x^2}{2\zeta_{nx}^*}-\frac{\beta_n p_y^2}{2\zeta_{ny}^*}\right)
$$

$$
+ \sum_{n=0}^{N}\sum_{n_1=0}^{n}\sum_{n_2=0}^{n_1}(-1)^{n_1}\binom{N}{n}\binom{n}{n_1}\binom{n_1}{n_2}\frac{\beta\alpha_{sx}^2\alpha_{sy}^2}{\left(\gamma_{nn_1n_2x}\gamma_{nn_1n_2y}\right)^{1/2}}\exp\left(\frac{\beta_{nn_1}\alpha_{sx}^2 p_x^2}{2\gamma_{nn_1n_2x}}+\frac{\beta_{nn_1}\alpha_{sy}^2 p_y^2}{2\gamma_{nn_1n_2y}}\right), \tag{14}
$$

where,

$$
\beta = k^2\rho_0^2,\ \ \beta_n = n\beta,\ \ \beta_{nn_1} = (n_1-2n)\beta,\ \ \zeta_{nx} = \left(\beta\alpha_{sx}^2 + 2L^2 n\right) + i\left(k\rho_0^2 Ln\right),
$$

$$
\gamma_{nn_1n_2x} = \beta\alpha_{sx}^4 + 2\alpha_{sx}^2 L^2\left(2n-n_1\right) + \rho_0^2 L^2\left(n-n_2\right)\left(n-n_1+n_2\right) + ik\rho_0^2\alpha_{sx}^2 L\left(2n_2-n_1\right),
$$

and $\zeta_{ny}, \gamma_{nn_1n_2y}$ are the y counterparts of $\zeta_{nx}, \gamma_{nn_1n_2x}$ in which x is replaced by y.

To examine the beam size variation along the propagation axis, Eq. (4) is employed, with the modification that in the numerator $I_s(\mathbf{s})$ is replaced with $I_r(\mathbf{p})$ from Eq. (14). Thus for the p_x direction, the beam size during propagation will be established as

$$
\alpha_{pxN} = \left[2\int_{-\infty}^{\infty}\int_{-\infty}^{\infty}p_x^2 I_r(\mathbf{p})\,dp_x dp_y \bigg/ P_{sN}\right]^{1/2}. \tag{15}
$$

Owing to the nature of turbulent atmosphere propagation, there exists no attenuation or absorption in the medium. Thus, we are able to retain the integrand in the numerator of Eq. (15) to be that of the source plane. Looking at Eq. (14), it is clear that due to the complexity of the expression for $I_r(\mathbf{p})$, we cannot proceed analytically; therefore numerical evaluations have to be sought for finding the beam size during propagation.

The kurtosis parameter of the propagating beam is defined as the ratio of the fourth and second moments of the intensity in the following way [18]

$$
K_x = \frac{\displaystyle\int_{-\infty}^{\infty}\int_{-\infty}^{\infty}p_x^4 I_r(\mathbf{p})\,dp_x dp_y\bigg/ P_{sN}}{\left[\displaystyle\int_{-\infty}^{\infty}\int_{-\infty}^{\infty}p_x^2 I_r(\mathbf{p})\,dp_x dp_y\bigg/ P_{sN}\right]^2}, \tag{16}
$$

K_y is found by switching the receiver plane coordinate parameter to p_y. Again, the complexity of the $I_r(\mathbf{p})$ expression does not allow us to acquire an analytic result for the kurtosis parameter.

Finally in this section, we state the power that will fall into a receiver aperture of radius α_r, which is also known as power in bucket, that is

$$P_{\alpha N} = 2\pi \int\limits_0^{\alpha_r} r I_r(\mathbf{p}) dr \bigg/ P_{sN}. \tag{17}$$

In dividing by the source power, P_{sN}, i.e. the term in the denominator of Eq. (17), it is envisaged that each individual FT beam of order N, is normalized with respect to its own order of flatness.

3. Results and discussions

3.1. Source plane

Taking Eq. (4), in Fig. 1, we initially plot the 3D picture of source intensity at fixed Gaussian source sizes of $\alpha_{sx} = \alpha_{sy} = 3$ cm, against the flatness order N. As seen in this figure, the source intensity of the FT beam will become flatter with escalating N values, eventually assuming the shape of a cylinder if equal Gaussian source sizes are used. Figure 1 also makes it evident that higher N values will give rise to larger beam sizes and source powers.
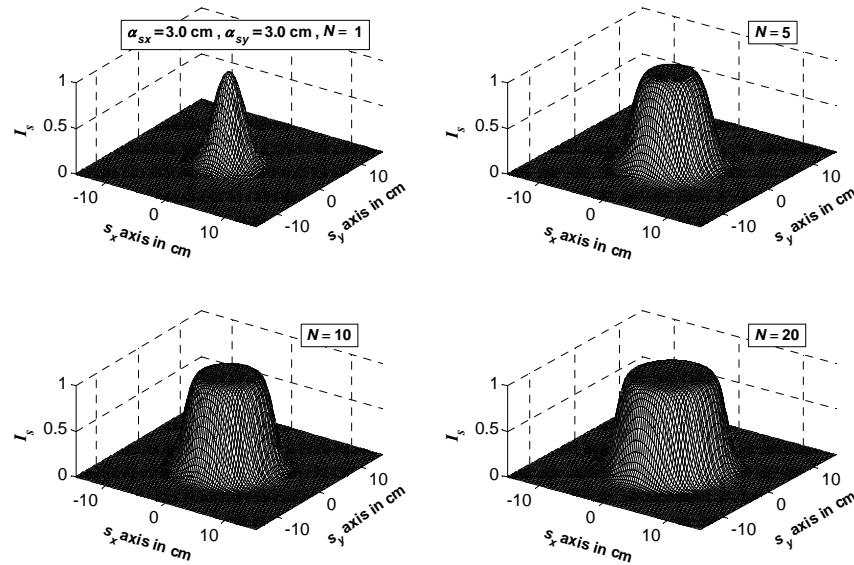
Fig. 1. FT source beam profiles at different flatness order.

Figure 2 contains the overlaid contour plots of the beams belonging to Fig. 1, cut along the slanted axis of the transverse plane. From Fig. 2, the increases in beam size and source power of the FT beam at higher values of N are detected once more.
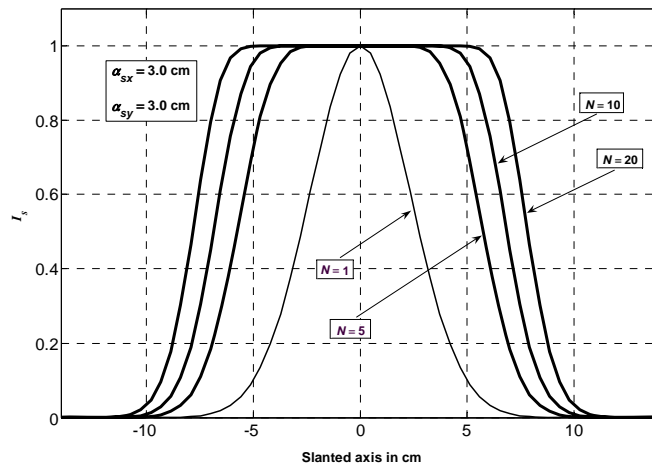
Fig. 2. Overlaid plots of four FT source beams belonging to Fig. 1 cut along the slanted axis.
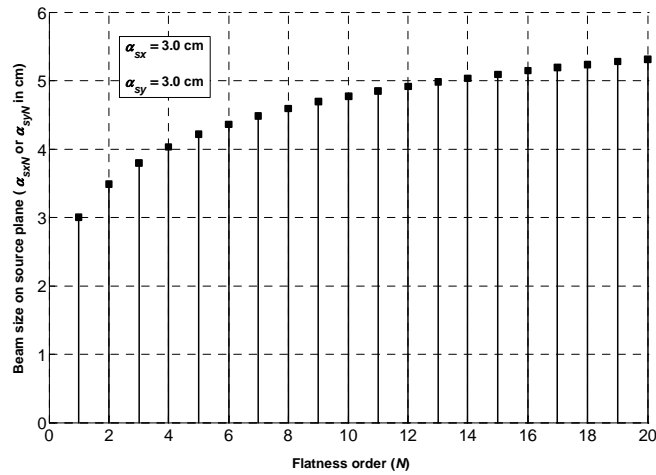

Fig. 3. Source beam size variation versus flatness order.

The observations in Figs. 1 and 2 about the variations of beam size and source power against flatness order N are in conformity with the associated mathematical formulations found in Eqs. (5) and (6). To assess these variations quantitatively, using Eqs. (5) and (6), Figs. 3 and 4 are plotted. Comparing Figs. 3 and 4, we conclude that the proportional increases in the source power against N, are more rapid than those of the beam size. It is to be understood from Figs. 3 and 4 that, to arrive at meaningful results for the receiver plane parameters, each FT beam must be normalized with respect to its own source plane parameters, rather than the normalization with respect to the Gaussian case for which N is unity.
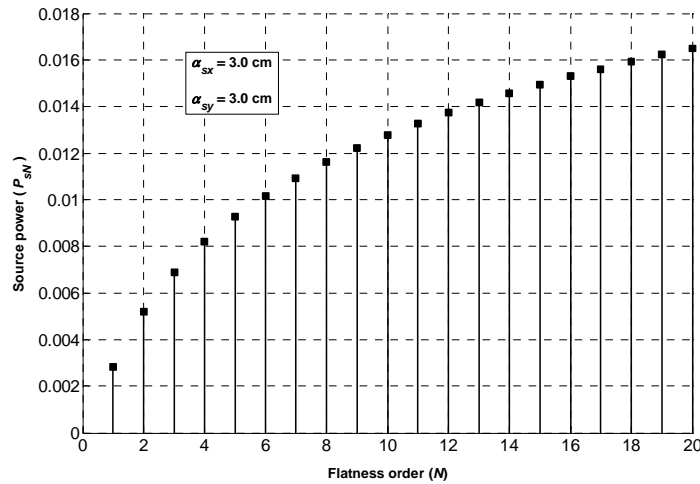
Fig. 4. Source beam power variation versus flatness order.

According to Fig. 5, M_x^2 factor will become larger as the flatness order increases. This finding is consistent with the results in Ref. 10.
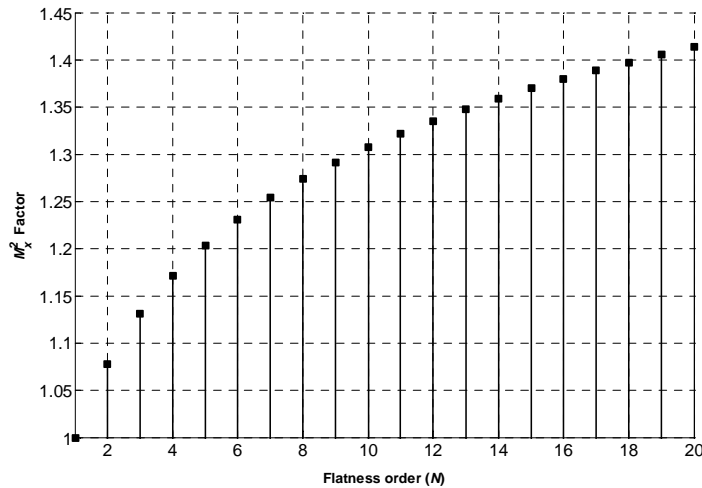

Fig. 5. Variation of M_x^2 versus flatness order.

3.2. Receiver plane

Throughout the receiver plane illustrations, we have utilized the wavelength and structure constant of $\lambda = 1.55\ \mu\text{m}$, $C_n^2 = 10^{-15}\ \text{m}^{-2/3}$. Therefore, these parameters are not quoted in our figures. By taking Eq. (14) and setting the source sizes and the flatness order as stated in the inset of the figure, Fig. 6 provides the views of the FT beam at selected propagation distances. Figure 6 shows that, the FT beam will initially develop a circular ring in the center. As the propagation advances, the circumference of this ring will become narrower, while a downward peak will gradually emerge from the center of the beam. Eventually this peak will smooth out the initial ring, with the profile turning into a pure Gaussian shape. This phenomenon may be considered to be akin to acquiring the spot of Arago as described in [19]. This type behavior of the FT beam is also commonly observed in other studies of free space

propagation [4, 7, 8, 9, and 11]. For the FT beam of Fig. 6, the overlaid views of the beam progress cut along the slanted axis are displayed in Fig. 7. Introducing the Fresnel parameter $F = \alpha_s^2 / (\lambda L)$ with $\alpha_s = \alpha_{sx} = \alpha_{sy}$ being the source size for a symmetrical source, in the plots of Figs. 6 and 7, the propagation distances of $L = 0.7$ km, 1.4 km and 5 km correspond to F of 0.83 (i.e., close to Fresnel diffraction region meaning near field), 0.42 and 0.12 (i.e., in the Fraunhoffer diffraction region meaning far field), respectively.
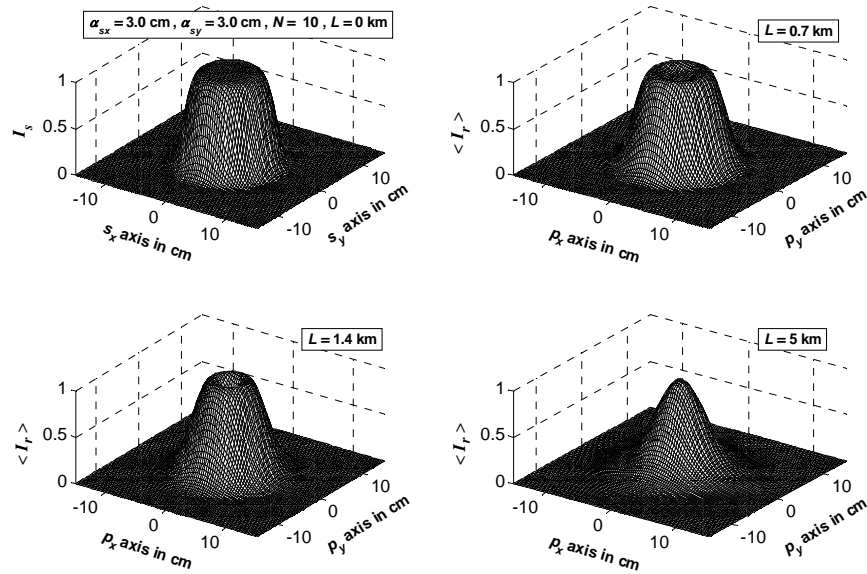
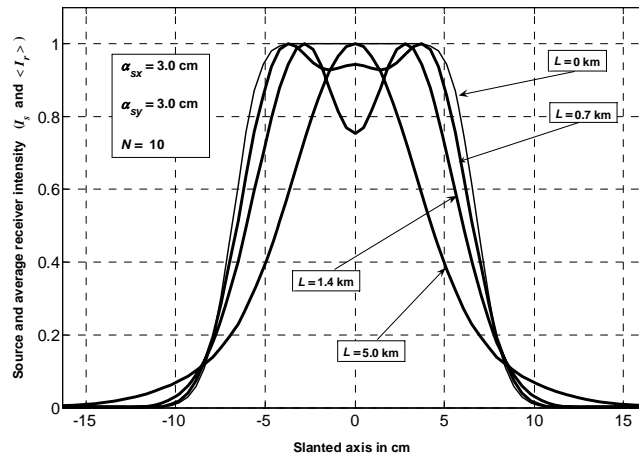Fig. 6. Propagation view of the FT beam for selected source and propagation parameters.

Fig. 7. Overlaid plots of the FT beam belonging to Fig. 6 cut along the slanted axis.

Upon choosing asymmetric source sizes, an elliptical source beam is accomplished [8]. Further we can create an FT beam with sharp edges by exaggerating this asymmetry feature. The receiver plane intensity of such a beam is offered in Fig. 8, along with the associated source plane intensity. Here, the effect of the propagation channel implementing a Fourier

transform action on the source beam field, thus converting it into an Airy function like shape in intensity during propagation, is slightly visible from the side lobes present in the lower picture of Fig. 8. Here we note that the most general case of elliptical flat-topped beam whose profile variables x and y cannot be separated is characterized by α_{sx}, α_{sy} and α_{sxy} as shown in Ref. [9]. The propagation of such astigmatic flat-topped beam in the turbulent atmosphere is recently reported by Cai and He [20, 21]. The elliptical flat-topped beam of our derivation is obtained by setting $\alpha_{sx} \neq \alpha_{sy}$.
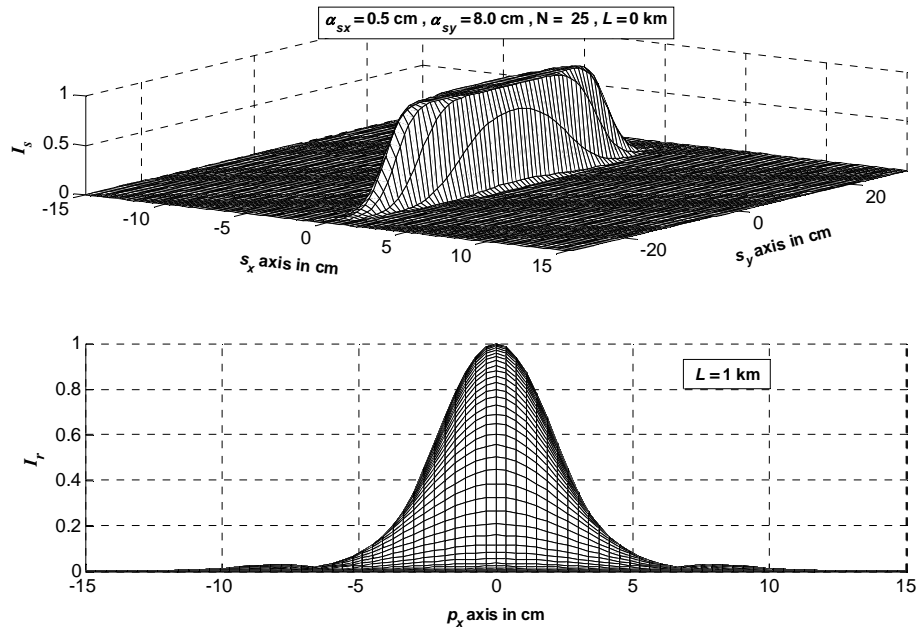

Fig. 8. Intensity distribution of an elliptical FT beam before and after propagation.
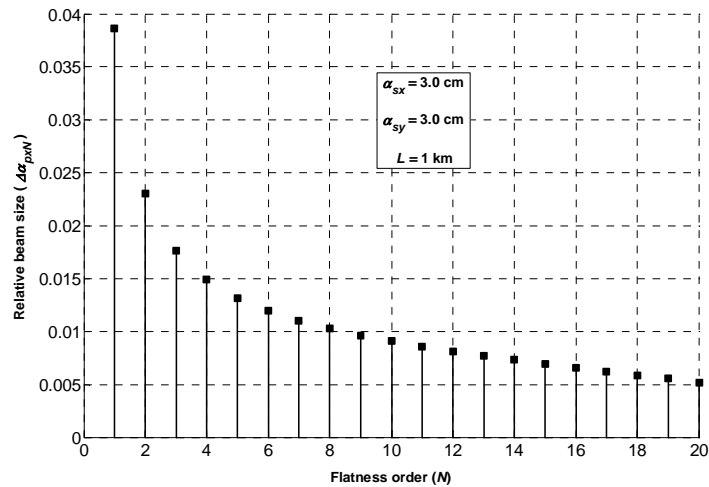

Fig. 9. Receiver beam size variation versus flatness order.

Next we explore the beam size and power in bucket variations along the propagation axis. The beam size variation is shown in Fig. 9 against the flatness order, where the Gaussian source sizes and propagation length are adjusted as given in the same figure Here for better

assessment, based on Eqs. (5) and (15), we have resorted to the relative beam size definition given by

$$\Delta\alpha_{pxN} = \left(\alpha_{pxN} - \alpha_{sxN}\right)/\alpha_{sxN}. \tag{18}$$

Figure 9 reveals that for the selected range of source and propagation parameters, the relative beam size drops sharply at lower values of N, while this trend later continues at much slower pace. Turning to power in bucket variation and choosing a receiving aperture size of $\alpha_r = 0.5\left(\alpha_{sx}^2 + \alpha_{sy}^2\right)^{1/2}$ in Eq. (17), we come across a similar picture, as illustrated in Fig. 10, where the falling trend at small N values is slightly retarded. Of course we should be careful here in the interpretation of receiving less power with increasing N. Less power occurs because, as explained underneath Eq. (17), $P_{\alpha N}$ is determined by dividing the received power of each individual FT beam by its own source power. If this normalization were to be carried out with respect the Gaussian case, i.e., $N = 1$, then we would come across rising power in bucket values with increasing N, instead of the presently falling trend.
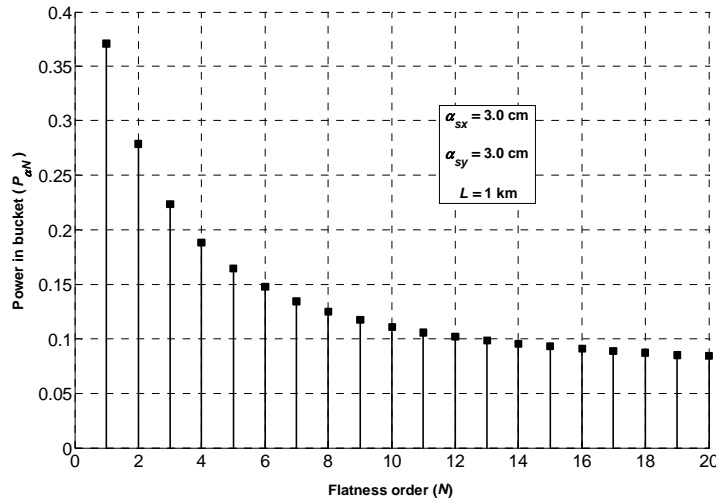

Fig. 10. Power in bucket variation versus flatness order.

Finally in this section, we analyze the kurtosis parameter which is known to be linked to the flatness or sharpness of the beam [18]. Figure 11 exhibits the variation of kurtosis parameter versus the propagation length at selected N values and fixed Gaussian source sizes. It is to be noted from Figs. (1) and (2) that on the source plane, the beam profile becomes sharper with larger N. This fact is reflected in Fig. 11 such that at short propagation distances, kurtosis parameter becomes smaller as N gets bigger. On the other hand, kurtosis parameter of all beams, except for $N = 1$, begins to rise at medium propagation ranges, later reaching a maximum. This is a predictable behavior, where the rise corresponds to the formation of the ring, the subsequent narrowing action and then the appearance of the peak in Figs 6 and 7. When these curly surfaces on the beam start to erode with the beam evolving towards a Gaussian profile, the kurtosis parameter declines, finally approximating to the $N = 1$ (Gaussian) case for all N values, as seen to the right of Fig. 11.
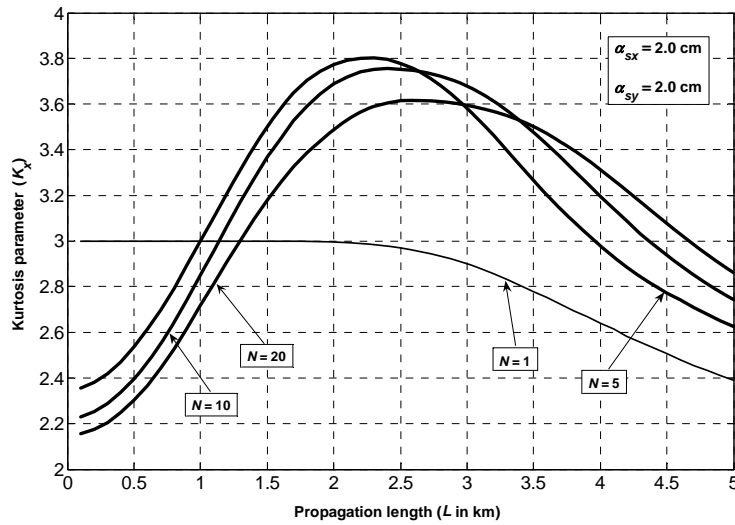
Fig. 11. Kurtosis parameter variation versus propagation length.

4. Conclusion

The source and receiver plane characteristics of flat topped (FT) beam propagating in turbulent atmosphere are studied. Source beam intensity, source beam size and power, M^2 factor are formulated and plotted against flatness order. From these plots, it is seen that beam intensity profile will become flatter, while source size, beam power and M^2 factor will increase against growing value of flatness order. Via the use of Huygens Fresnel integral, the average intensity on the receiver plane for a turbulent propagation environment is derived. Based on this intensity expression, the kurtosis parameter, beam size variation along the propagation axis and power in bucket formulations are stated. Plotting the receiver average intensity at selected source and propagation parameters, it is observed that, initially a circular ring will be formed in the center. As we go along the propagation axis however, the circumference of this ring will become narrower, while a downward peak will gradually emerge from the center of the beam. Eventually this peak will smooth out the initial ring, with the profile converging towards a pure Gaussian shape. These beam profile changes are also reflected in the plots of kurtosis parameter against propagation length. Furthermore, when the source beam is made highly asymmetric, the conversion of receiver intensity profile into an Airy function becomes more visible. The relative beam size becomes smaller, as the order parameter is raised, indicating that flatter beams will be subjected to less spreading during propagation in turbulence. For a fixed receiver aperture radius, less power is captured against the rising flatness order.